Biomaterials Science

PAPER

View Article Online
View Journal | View Issue

Cite this: *Biomater. Sci.*, 2019, **7**, 3041

Monitoring ^{111}In-labelled polyisocyanopeptide (PIC) hydrogel wound dressings in full-thickness wounds†

Roel C. op 't Veld, [a,b] Lieke Joosten, [c] Onno I. van den Boomen,[d,e] Otto C. Boerman, [c] Paul Kouwer, [d] Esther Middelkoop, [f,g] Alan E. Rowan, [d] John A. Jansen,[a] X. Frank Walboomers [a] and Frank A. D. T. G. Wagener *[b]

Wounds often result in scarring, prolonged morbidity, and loss of function. New interactive and modifiable hydrogel wound dressings are being developed for these injuries. Polyisocyanopeptide (PIC) gel is a promising thermosensitive hydrogel having several characteristics that can facilitate wound repair, including ease of application/removal and strain-stiffening properties that mimic extracellular matrix components. However, it is unknown whether the PIC gel remains in the wound for a clinically relevant time period. Therefore, PIC polymers were functionalized with a DTPA group allowing labelling with Indium-111 (^{111}In). Following application of this radiolabelled gel to splinted and non-splinted murine full-thickness skin wounds the signal was monitored using SPECT/CT imaging for 7 days. The SPECT signal from the PIC gel was highly stable and covered the complete wound area. Non-bound ^{111}In-EDTA was rapidly cleared *via* the kidneys to the urine. The impact of PIC gels on wound repair was further studied visually and histologically. Radiolabelled PIC gel was observed to move both over and under the skin, while histological analysis demonstrated that part of the gel became encapsulated within the wound repair tissue, but did not delay wound closure or otherwise impair wound healing. This work illustrates for the first time the use of ^{111}In-labelled PIC gels for diagnostic and monitoring purposes and describes the use of PIC in the (non-)splinted murine skin wound model. It was found that PIC gels remained in splinted and non-splinted full-thickness skin wounds during wound repair. This warrants the continuation of developing the PIC gel into a clinically advanced wound dressing.

Received 25th April 2019,
Accepted 14th May 2019

DOI: 10.1039/c9bm00661c

rsc.li/biomaterials-science

1. Introduction

The management of complicated wounds, such as pressure/diabetic ulcers and burns, takes a significant amount of health care resources. Burn wounds are a leading form of household injuries, often involving infants, and are particularly dominant in low-income areas. These injuries result in 18 million disability adjusted life years (DALY's) worldwide.[1,2] Treatment of burns involves dressing the wound with products, which are often expensive and complicated to use. Considering the amount of personal care these patients require the daily costs of the management of these wounds is considerable.[3] Yet, most products are tedious and difficult to apply and remove and may include fibres that can become integrated in the wound bed. Removal is often painful and disturbs the healing process, which further contributes to patient discomfort and noncompliance.[4] Thus, there is an urgent need for more versatile products for wound management.

In general, hydrogel wound dressings are ideal for low-exudating or dry wounds and can be more conveniently applied around joints.[5,6] The large amounts of water present in these gels can aid in moist wound healing, which is often associated with enhanced re-epithelialization.[7] Furthermore, the polymer materials composing these hydrogels tend to have additional benefits such as inherent antibacterial or anti-oxidant

[a]*Division of Biomaterials, Department of Dentistry, Radboud University Medical Centre, Nijmegen, the Netherlands*
[b]*Division of Orthodontics and Craniofacial Biology, Department of Dentistry, Radboud University Medical Centre, Nijmegen, the Netherlands. E-mail: Frank.Wagener@radboudumc.nl*
[c]*Department of Radiology and Nuclear Medicine, Radboud University Medical Centre, Nijmegen, the Netherlands*
[d]*Department of Molecular Materials, Institute for Molecules and Materials, Radboud University, Nijmegen, the Netherlands*
[e]*Noviocell BV, Oss, the Netherlands*
[f]*Association of Dutch Burn Centres, Red Cross Hospital, Beverwijk, the Netherlands*
[g]*Amsterdam UMC, Vrije Universiteit Amsterdam, Department of Plastic, Reconstructive and Hand Surgery, Amsterdam Movement Sciences, Amsterdam, the Netherlands*

†Electronic supplementary information (ESI) available. See DOI: 10.1039/c9bm00661c

properties.[8–10] Recently, polyisocyanopeptide (PIC) hydrogels were presented as a potential new hydrogel wound dressing.[11] These synthetic gels stiffen when they are stretched, an effect called strain-stiffening, which is typically only seen in gels of natural polymers such as extracellular matrix (ECM) components.[12,13] PIC hydrogels are thermosensitive; they form low-viscous aqueous solutions at low temperatures that gelate when heated above the gelation temperature around 18 °C. When sprayed or poured onto a wound, the body heat is sufficient to induce gelation, which facilitates application in complicated areas such as near fingers or joints. The gel is capable of supporting its own weight even at extremely low concentrations, which indicates it can adhere sufficiently in animal models.[12] The thermal gelation is completely reversible, which allows for smooth pain-free removal or replacement of the PIC gel, simply by rinsing the wound bed with slightly cooled saline or tap water and physically flushing the polymer solution out of the wound. In addition, the modifiable PEG side-groups of PIC allow for functionalization for therapeutic or diagnostic purposes.[14,15] Previous studies have shown that the PIC gel is mesoporous[12,16] and that the presence of granulocytes is reduced when wounds are treated with PIC.[11] These results implied that PIC gel dressings have the potential to form a physical barrier against micro-organisms and could reduce the risk of infection. Furthermore, it was found in an earlier *in vivo* study that it was challenging to locate the gel several days after application, due to active movement and grooming of the mice. It is important that PIC wound dressings stay in place for two reasons: (1) the gel should not relocate to distant locations in the body, where it may cause side-effects, and (2) the PIC gel is unable to offer some of its potential benefits (*e.g.* hydration and protection) when it does not remain in the wound. A method to accurately trace and monitor the presence of PIC hydrogel in the wound and the rest of the body is thus desired.

In this work, we prepared PIC hydrogels radiolabelled with ^{111}In and use single-photon emission computed tomography (SPECT) imaging[17–19] to non-invasively monitor the distribution of PIC in the body after topical application on full-thickness wounds over the course of one week. To this end, we have modified our wound model in mice compared to our previous study.[11] Murine cutaneous wounds predominantly close by contraction of the subcutaneous muscle layer (*panniculus carnosus*) in favour of re-epithelialization and myofibroblast contractile activity.[20] Therefore, we use a "humanized" model that involves gluing a ring-shaped silicone rubber splint around the wound, which inhibits contraction and will thus more accurately represent human wound healing and clinical wound care.[21,22] In addition, we applied a secondary dressing to prevent the mouse from removing the PIC gel and splints from its wounds. This is a proof-of-principle study that investigates the use of PIC wound dressings in a controllable full-thickness wound model, prior to moving to a more complicated model such as a burn injury.

The aim of the study was to investigate the biodistribution of ^{111}In-labelled PIC wound dressings using SPECT/CT and whether or not a sufficient amount remains inside the wound area. Secondary objectives include characterizing the histological wound bed at 7 days post wounding, as well as gaining new insights into the use of a humanized full-thickness murine wound model that includes treatments with gel dressings that are supported by a secondary dressing and comparing splinted to non-splinted wounds. Based on the stability of the PIC polymer and previous results, we hypothesized that PIC gels were stable in the wound up to 7 days post application and were not absorbed and transported to distant locations in the body. The goal of this study is to investigate whether PIC wound dressings can keep the wound covered for a clinically relevant time.

2. Materials and methods

2.1 Synthesis of PIC-$(DTPA)_{0.01}$ and labelling with ^{111}In

The 1%-azide-functionalized PIC polymer (PIC-$(N_3)_{0.01}$) was prepared as was described previously.[12,15] The synthesis of PIC-$(DTPA)_{0.01}$ and insertion with ^{111}In is shown in Fig. 1 and the methods and characterization are described in more detail in ESI S1.† Mechanical analysis of different batches PIC-$(DTPA)_{0.01}$ gels (2 mg ml^{-1} in MilliQ water) gave storage moduli (G') between 150 and 200 Pa at 37 °C and a sol-to-gel transition temperature of 18 °C, in line with other PIC gels. All experiments described in this article were performed using DTPA-functionalized PIC. To introduce the radiolabel, a PIC-$(DTPA)_{0.01}$ solution (6.5 mg ml^{-1}) in 0.5 M metal-free 2-(*N*-morpholino)ethanesulfonic acid (MES) buffer, pH 5.0 (Sigma Aldrich, Zwijndrecht, the Netherlands) was prepared and was stored at −20 °C three days prior to labelling. The PIC-$(DTPA)_{0.01}$ solution was thawed at room temperature and $^{111}InCl_3$ in HCl (0.814 MBq μl^{-1}) was added to 185 μl of this solution, resulting in an activity of 57 MBq. After incubation at 4 °C for 3 hours, 50 mM ethylenediaminetetra-acetic acid (EDTA, Sigma Aldrich) was added to a final concentration of 5 mM to complex unincorporated ^{111}In. The resulting ^{111}In-PIC solution was diluted to 4 mg ml^{-1} with 0.25 M PBS (Sigma Aldrich). Furthermore, unlabelled PIC-$(DTPA)_{0.01}$ solution from the same stock was diluted with PBS to 4 mg ml^{-1}. The labelling efficiency was determined by spin column size exclusion separation (Amicon® Ultra-0.5 Centrifugal Filter devices, Sigma Aldrich) with a 3000 nominal molecular weight limit filter by centrifuging at 14 000 rpm (~20 000*g*) at room temperature for 25 minutes.

2.2 Animals

Ten female C57BL/6N mice of 6-to-8 weeks of age (Charles River, Sulzfeld, Germany) were housed individually with water and food *ad libitum* and a 12 hours day/night cycle for the main experiment. Four mice were used under the same conditions for pilot experiments (data not shown). The experiments were performed with permission of the Animal Ethical Committee of Radboud University, Nijmegen, the Netherlands (DEC 2014-208) and were in accordance with national guide-

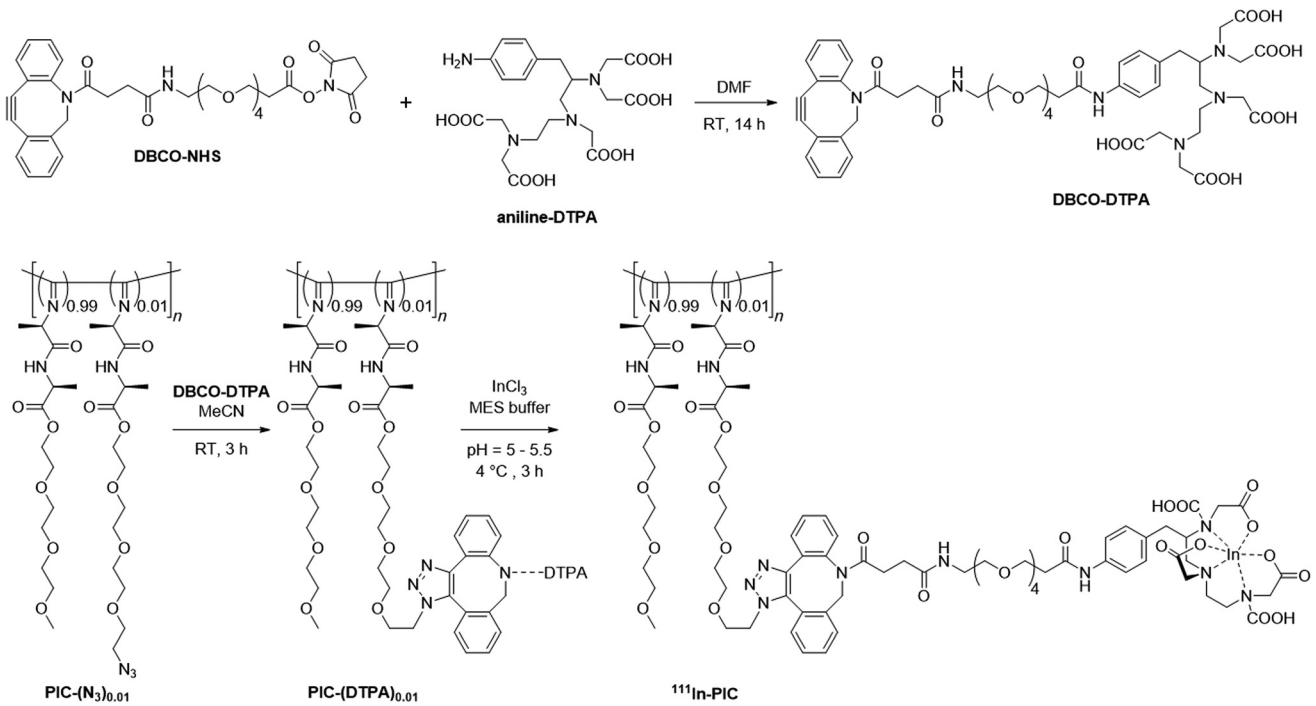

Fig. 1 Synthesis of PIC-(DTPA)$_{0.01}$ and labelling with $^{111}InCl_3$ to form '^{111}In-PIC'. After conjugation of PIC gel with the DTPA group its colour changes from a yellow-brown (Azide-PIC) to dark brown (DTPA-PIC) (see ESI S1†).

lines (Experiments on Animals Act; 'Wet op dierproeven', 2014) and international standards defined by the European Union (European Directive; 2016/63/EU). All housing and experiments took place in the Central Animal Facility Nijmegen, the Netherlands.

2.3 (Non-)Splinted full-thickness wound model and treatment

Mice were anesthetized using an evaporated isoflurane/air mixture. The dorsal skin was shaved and disinfected with Betadine (Meda Pharma B.V., Amstelveen, the Netherlands). A fold of skin was pinched and stretched along the dorsal midline, just below the shoulders. A 4 mm diameter biopsy punch (Kai Medical, Seki, Japan) was punched through the folded skin to create two identical full-thickness wounds. Then, a ring splint made from silicone rubber (inner ∅ 6 mm, outer ∅ 12 mm, 0.5 mm thick) (Rubbermagazijn, Zoetermeer, the Netherlands) was glued in place around the wound using cyanoacrylate glue (Bison International B.V., Goes, the Netherlands). Five mice received 20 μl of ^{111}In-PIC on their splinted right wound and 20 μl of unlabelled PIC-(DTPA)$_{0.01}$ on their splinted left wound (group A). The remaining five mice received 20 μl of ^{111}In-PIC on their right wound, but this wound remained non-splinted, while their left wound remained untreated but with a splint (group B). These volumes were determined by calculating the rough volume of the wound (12.6 μl assuming a thickness of up to 1 μm) and applying PIC gel in an excess (20 μl). The activity dose applied to these right wounds was 4.3 ± 0.2 MBq. After gelation had occurred (~1 minute), wounds were covered with a 4.4 × 4.4 cm sheet of Tegaderm™ (3 M Healthcare, Diegem, Belgium) and the dorsal/ventral sides were wrapped securely with a bandage (Petflex®, Andover Healthcare Inc., Salisbury, MA). The surgical procedure is highlighted in ESI Fig. S2.† Photographs of the wounds were taken right after application (day 0) and at the end of the experiment after euthanasia of the animals (day 7).

2.4 SPECT/CT imaging

SPECT/CT images were acquired on day 0 (immediately after surgery) with an acquisition time of 20 minutes and on days 1, 3 and 7 after surgery with an acquisition time of 40 minutes, using a 1.0 mm pinhole mouse collimator in a dedicated small animal SPECT/CT scanner (U-SPECT-II, MILabs, Utrecht, the Netherlands). SPECT images were reconstructed with Ordered Subset Expectation Maximization (OSEM) (3 iterations, 16 subsets, voxel size 0.4 mm) with U-SPECT-Rec software (MILabs). CT scans were performed with spatial resolution 160 μm, 65 kV, 615 μA.

2.5 Biodistribution

After the final SPECT/CT image acquisition 7 days post-surgery, mice were euthanized by suffocation with CO_2/O_2. Wounds and a section of dorsal control skin were retrieved using a biopsy punch (Ø 6 mm). Relevant tissue samples (blood, muscle, heart, lung, spleen, pancreas, kidney, liver, stomach and duodenum) were dissected, weighed and counted in a 2480 WIZARD^2 Automatic Gamma Counter

(PerkinElmer®, Groningen, the Netherlands) along with a 1% standard to determine the injected dose per gram tissue (%ID g^{-1}).

2.6 Histology

Harvested skin samples were fixed in 4% formalin at room temperature for 24 hours and then moved to 70% ethanol and stored at 4 °C for roughly 18 hours prior to embedment in paraffin using a Leica TP1020 tissue processor (Leica Microsystems B.V., Amsterdam, the Netherlands) and a Tissue-TEK TEC (Sakura Finetek Europe B.V., Alphen aan den Rijn, the Netherlands). Sections (5 μm) were cut with a Microm HM335E microtome (GMI Inc., Ramsey, MN) and mounted on microscope slides (Superfrost™, Thermo Fisher Scientific, Landsmeer, the Netherlands). Haematoxylin and Eosine (H&E) stainings were performed according to Delafield protocol. Immuno-histological stainings were performed as described previously.[11]

2.7 Wound size, SPECT quantification and histological analysis

Photographs of wound sites were analysed for wound size at day 0 and 7 using ImageJ software (v1.151 h).[23] Images were set to scale using a ruler, the wound edge was delineated and the surface area of the wound was calculated. Finally, the surface area on day 7 was expressed as a percentage of the surface area on day 0.

SPECT images were analysed with Inveon Research Workplace (Siemens Healthcare, The Hague, the Netherlands). The amount of ^{111}In-PIC activity in the wound area was determined by quantitative analysis of the SPECT/CT images obtained on day 0, 1, 3 and 7. The activity in the right wounds was determined by drawing a 6 mm diameter sphere-shaped region of interest (ROI) centred in the wound. The same shape was placed in an empty ROI that was void of any tissue or other structures to determine the background signal, and this value was deducted from the wound signal. Finally, this intensity was corrected for physical decay and expressed as a percentage of the signal on day 0. Whole body activity was determined by positioning a cylinder-shaped region of interest from the neck to the tail-base on the CT scan. A threshold of 99.9% of CT signal was set and the region of interest was copied to the SPECT image in order to omit empty space in the measurement. The whole body activity was corrected for background signal, physical decay and expressed as percentage of signal on day 0.

Histological sections were scanned using a Pannoramic P250 digital slide scanner (3DHISTECH Ltd, Budapest, Hungary). Images were digitally viewed and cropped at 5× zoom level using Pannoramic Viewer software (v1.15.4, 3DHISTECH Ltd) for display in this article. Histological investigation was performed live with a Leica DM LB microscope at variable zoom levels by authors R.C.V. and F.A.D.T.G.W. In H&E sections, whole wound sections were investigated to count the number of giant cells and it was noted whenever hydrogel was visible.

2.8 Statistical analysis

For wound and whole-body activity measurements the time points were compared with paired sample *t*-tests and groups were compared with independent sample *t*-test. In wound contraction analysis independent sample *t*-test was utilized. For all tests a p-value <0.05 was considered statistically significant.

3. Results

3.1 Synthesis of PIC-$(DTPA)_{0.01}$ and labelling with ^{111}In

The preparation of radiolabelled ^{111}In-PIC is outlined in Fig. 1. In brief, aniline-DTPA is equipped with a dibenzoazacyclooctyne (DBCO) group compatible with a strain-promoted azide-alkyn coupling reaction. PIC polymers with 1% azide functional groups were prepared as described previously[12,15] and conjugated with the DBCO-DTPA group. Earlier, we described the high efficiency of the SPAAC reaction (strain-promoted azide–alkyne cycloaddition) in this conjugation of small[14] and large (bio)molecules.[24] PIC-$(DTPA)_{0.01}$ displayed similar thermosensitive gelation behaviour and mechanical properties as the previously described PIC gels (see ESI S1†). Then, PIC-$(DTPA)_{0.01}$ was stirred with an excess of $^{111}InCl_3$ to introduce the radiolabel. The labelling efficiency was determined by spin column separation using a centrifuge; labelled polymers became stuck in the column while the comparably small ^{111}In-EDTA passed through to the collection tube. This efficiency was estimated to be around ~40% using the aforementioned labelling method.

3.2 SPECT/CT imaging and biodistribution

All animals survived the treatment until the final day, no complications were observed although the treatment was considered stressful and one developed a stomach ulcer. Analysis of the SPECT/CT scans in 3D indicated that a portion of the ^{111}In signal came from the wounds, but a larger part resided in the surrounding skin topically. ^{111}In-PIC gel accumulated in spots underneath the secondary dressing, typically at the height of the shoulders or lower back, where the edge of Tegaderm™ dressing was located. Snapshots of 3D SPECT/CT images are presented in Fig. 2. Animated 3D images of SPECT/CT scans can be found in the ESI Videos S3.†

The ^{111}In-activity in the ^{111}In-PIC treated wounds and the whole body was quantified and the results are summarized in Fig. 3. In the first 24 hours activity in the wounds dropped rapidly and was then stable from days 3 to day 7 (Fig. 3A). The background activity was deducted from these measurements, which means any remaining activity may be attributed to the ^{111}In label. Most of the variability obtained here was the result of deviation between wounds, rather than within wounds. No statistical differences were noted in splinted and non-splinted wounds on day 1 compared to day 3, day 3 to 7, and day 1 to 7 ($p > 0.05$). The same was observed for measurements taken in the whole body ($p > 0.05$) (Fig. 3B). Total activity in the body was four times higher than activity in the wounds, due to accumulation of ^{111}In-activity beneath the secondary dressing. In addition, the activities were compared between splinted and

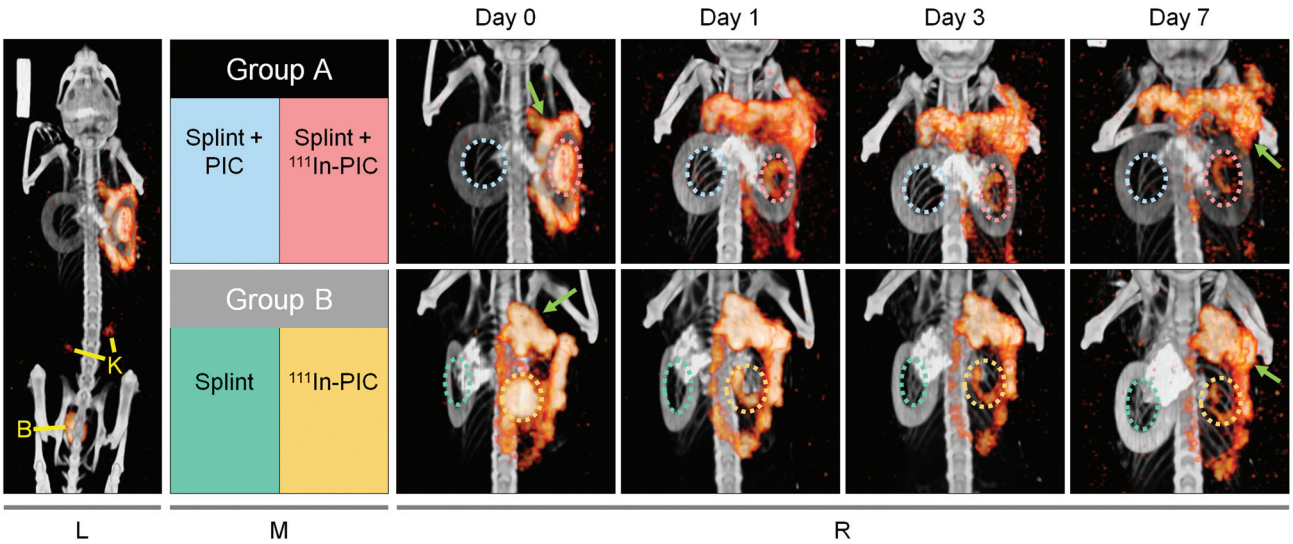

Fig. 2 Representative SPECT/CT images for mice from group A and B (n = 5 per group). The anatomy and splints are visible in grayscale (CT scan) and radioactive signal in colour scale (SPECT scan). The ring splints (grey circles) can be used as a scale (inner diameter of 6 mm and outer diameter of 12 mm). On the day 0 overview scan (left panel (L)) SPECT signal from ^{111}In-EDTA in the kidneys (K) and bladder (B) can be observed. The coloured boxes (middle panel (M)) describe the different treatment conditions indicated by dashed circles in the "zoomed-in" SPECT/CT scans (right panels (R)). The top panels in R display "Group A" in which both wounds have a splint, the right wound was treated with ^{111}In-PIC gel and left with (unlabelled) PIC-$(DTPA)_{0.01}$ gel. The bottom panels in R show "Group B", where the left wound is not treated with gel (but still has a splint) and the right wound has ^{111}In-PIC but is non-splinted. Green arrows indicate several examples of activity that leaked away from the wound area.

non-splinted wounds on day 1, 3 and 7 but no significant changes ($p > 0.05$) were detected. In the measurement of activity in dissected tissues a minor amount of activity was detected in the blood (0.032 ± 0.044 %ID g^{-1}), spleen (0.018 ± 0.003 %ID g^{-1}), kidneys (0.157 ± 0.021 %ID g^{-1}), and liver (0.017 ± 0.004 %ID g^{-1}) (Fig. 3C). High activity levels were detected in the ^{111}In-PIC treated wounds (*i.e.* right wounds), but also the left wounds (that were not treated with label-bearing gel) and healthy local control skin showed elevated activity.

3.3 Wound closure

Visually, the wound edges appeared to have joined at day 7, with epithelial migration still in progress. A mass of PIC hydrogel was found to remain in the wounds while another portion had migrated out and got stuck in the hairs at the border of the shaved area. The Tegaderm™ sheet adhered tightly to the skin, even after 7 days, and also contained traces of PIC gel when removed from the animal. Typical wounds and the rate of wound closure are depicted in Fig. 4. The non-epithelialized area of the non-splinted ^{111}In-PIC-treated wounds was not significantly smaller on day 7 compared to the splinted ^{111}In-PIC-treated wounds ($p > 0.05$). Noteworthy is that splints detached when removing the Tegaderm™ dressing and thus photographs for wound size analysis were taken when the skin was in a relaxed non-splinted state.

3.4 Histological analysis

Skin sections harvested on day 7 were H&E stained to study the general morphology and the presence of PIC gel in the wounds. It was observed that, in general, wounds healed as normal with epithelial migration having occurred in both splinted and non-splinted wounds. PIC gel could be identified in 75% of all samples, mostly lying topically on the wound. In many of the wounds, the PIC gel was encapsulated, forming one or several compartments in the wound repair tissue and sometimes reached shallowly into adjacent healthy skin layers. Moreover, gel was even identified in two untreated control wounds. It was observed that every treatment had samples both with and without encapsulated gel. No giant cells were observed, indicating the absence of a foreign body response. Representative histological H&E-stained sections are depicted in Fig. 5. In addition, SPECT/CT images highlighting the movement of ^{111}In-PIC both under and over the skin are shown in ESI Fig. S4.† Immuno-histological analysis was performed in a similar fashion as our previous study.[11] However, due to multiple control wounds being cross-contaminated with PIC gel we were unable to draw conclusions from these data. Worthy of note was that one wound in the splinted PIC gel group showed elevated granulocytic marker expression, which may have been indicative of an infection (see ESI Fig. S5).†

4. Discussion

The aim of this study was to non-invasively monitor ^{111}In-labelled PIC hydrogel wound dressings in a mouse model with full-thickness skin injuries. The conjugation of PIC with DTPA and labelling thereof with ^{111}In was successful. In order to

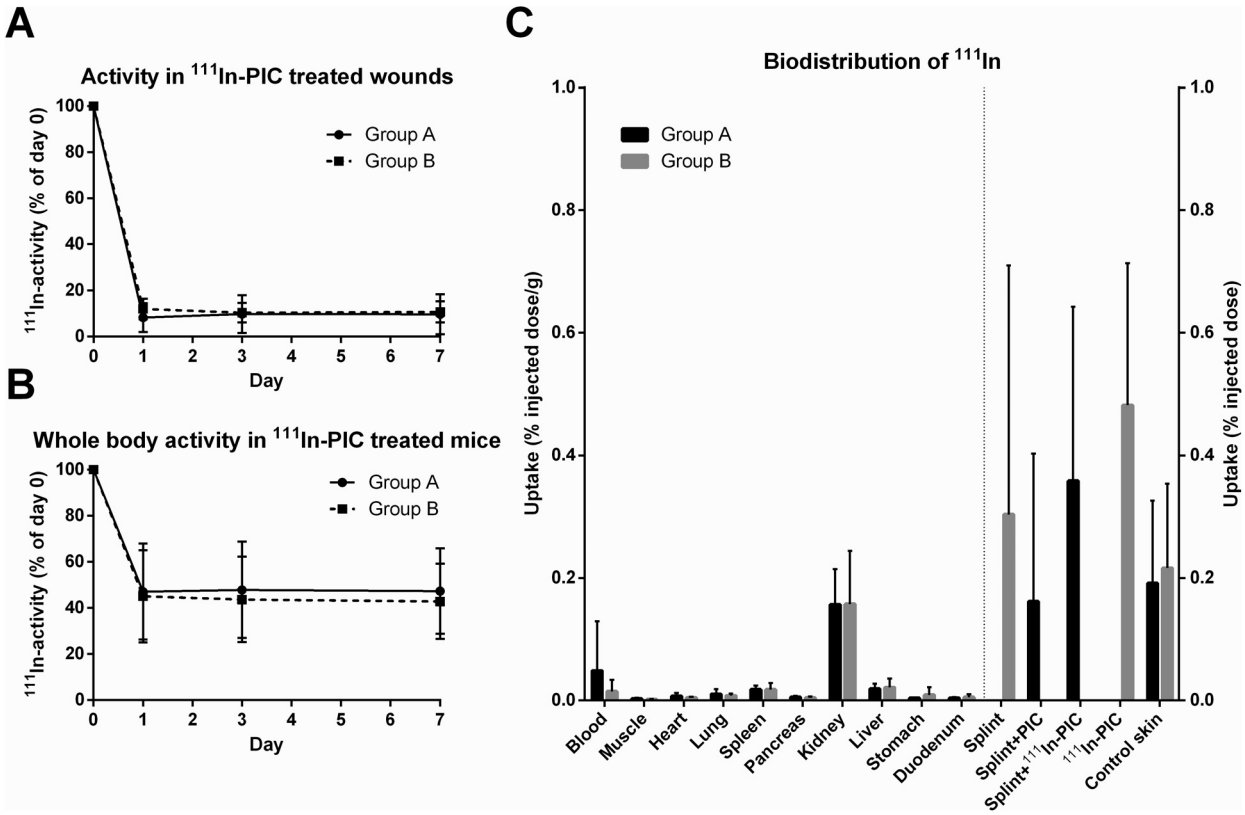

Fig. 3 Quantification on days 0, 1, 3 and 7 of ^{111}In in the (A) ^{111}In-PIC treated wounds and (B) whole body of these mice, as measured by SPECT/CT, corrected for physical decay of the radionuclide and expressed as percentage of the activity applied at day 0. A large drop in activity was seen during the first 24 hours. This loss can be attributed to ^{111}In-EDTA and the excess of PIC gel volume leaving the wound area. The remaining amount of activity present in the wound was stable from day 1 to 7 and can be assumed to originate from indium that is immobilized on PIC. (C) Post-mortem biodistribution analysis reveals elevated ^{111}In uptake in the blood, spleen, kidneys, and liver. Data for organs was expressed as percent of applied activity per gram of tissue (left of dotted line), while activity in wounds and control skin was expressed as percent of applied activity (right of dotted line). Note that the samples displayed to the right of the dotted line all represent a 6 mm diameter piece of excised skin which is either a treated wound or a control skin sample. The explanation of treatment groups can be found in the description of Fig. 2.

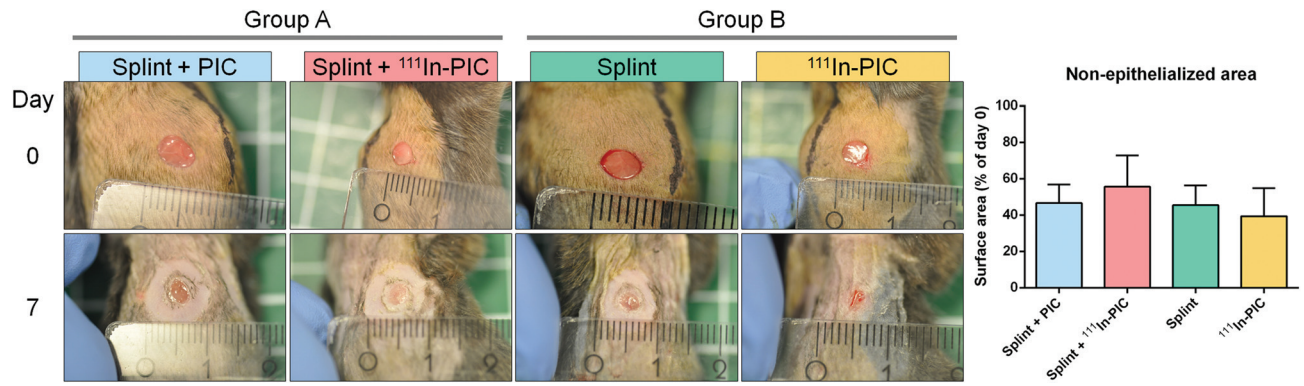

Fig. 4 Wounds 7 days post-surgery. It can be observed that splinted wounds close in a circular shape, whereas the non-splinted wounds contract in a characteristic oval shape. Wound edges connected and the non-epithelialized areas were of comparable size in all four treatments at 7 days post-surgery compared to the total wound size at day 0.

confirm whether PIC gel can be maintained as wound dressing for at least 7 days, the wounds were imaged using SPECT/CT imaging, photography, and histology. It was demonstrated that a continuous PIC gel layer remained in the wounds during this period, although a fraction was encased inside the wound tissue.

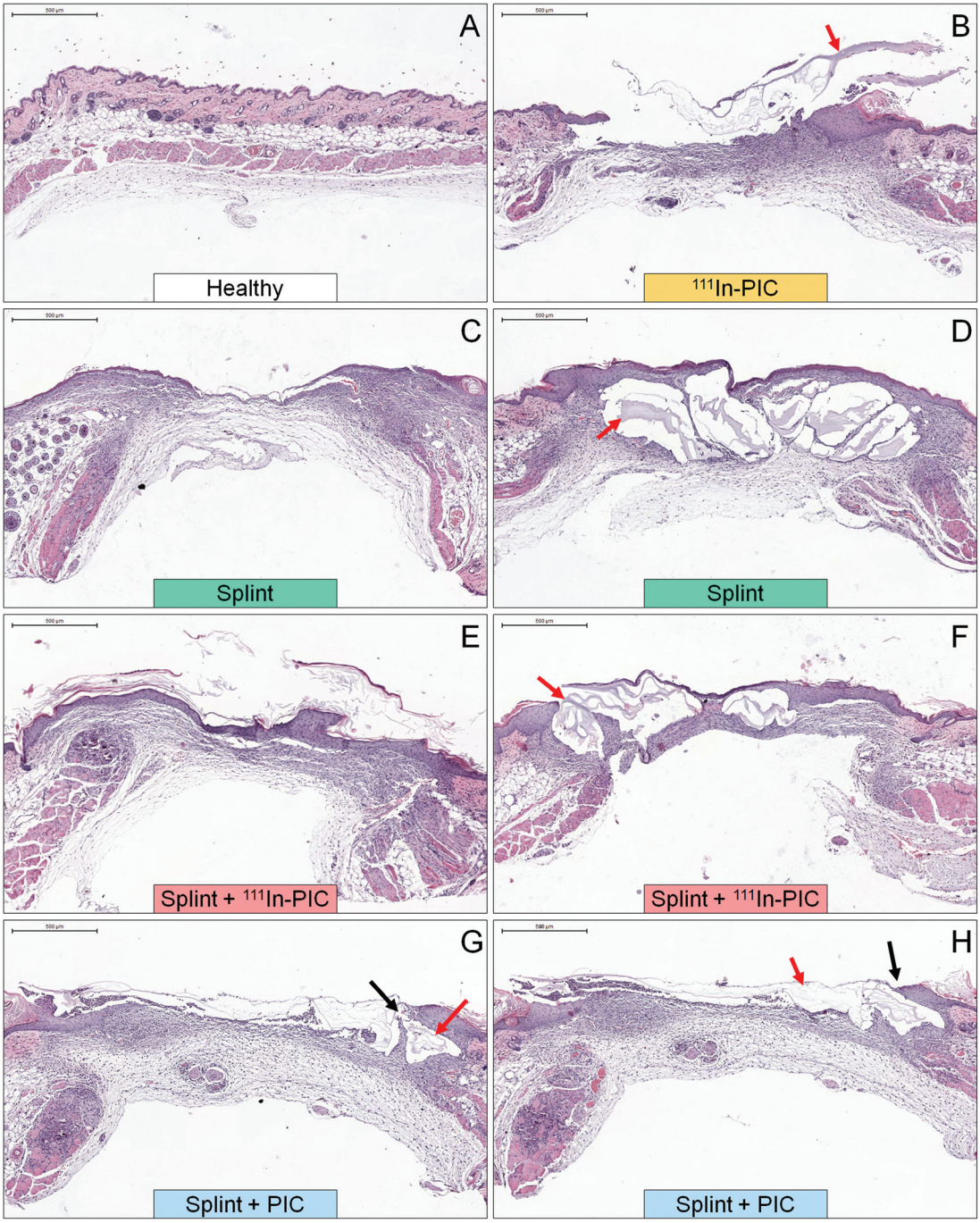

Fig. 5 The encapsulation of PIC gel in wound tissue at day 7. Red arrows indicate remnants of PIC gel. (A) A healthy skin section showing the undamaged structures of murine skin. (B) In ^{111}In-PIC treated wounds without a splint the epithelial layer is thick and gel is visible topically. (C) In splinted control wounds repair can be observed as normal. (D) In several control samples, PIC gel from the other wound translocated into the splinted control wound and becomes encased within the wound repair tissue. The compartments appear larger due to shrinkage of the gel during histological processing. In sections of splinted wounds treated with ^{111}In-PIC gel the gel is sometimes absent (E) and in other cases present (F). (G and H) The migration of epidermal cells over a volume of gel can be observed in two proximal sections of a splinted wound treated with PIC gel (indicated with black arrows). Scale bars represent 500 μm.

In a pilot study it was confirmed that PIC-$(DTPA)_{0.01}$ gels could be labelled efficiently with ^{111}In and could be detected in mice using SPECT/CT (results not shown). Labelling efficiency was 40% as determined by spin column separation, which indicates that 40% of the ^{111}In activity was incorporated in PIC and the remaining 60% was chelated in EDTA. Furthermore, we found that because of the physical decay of indium it was not worthwhile to continue any observation

beyond ~7 days as the signal becomes too weak to measure accurately. Because signals were still detectable after 6 days of treatment, it was concluded that ^{111}In-labelled PIC gels are stable enough to monitor for at least one week.

Subsequently, ten mice were treated and the SPECT/CT images were studied to monitor the behaviour of the ^{111}In-PIC in the mice in detail. At 24 hours after application a sharp drop in activity was observed in the wounds. This can be attributed to ^{111}In-EDTA that is rapidly absorbed and cleared to the urine as well as ^{111}In-PIC gel that moves out of the wound. In fact, day 0 scans show high activity in the kidneys and bladder. The free ^{111}In-EDTA was absorbed and cleared, whereas the remaining signal in the wounds originated from the ^{111}In-labelled-PIC gel. Whole body activity measurements of the mice indicated the portion that remained in the body. This turned out to be 46% and was similar to the fraction of activity associated with the PIC gel. The activity remaining in splinted and non-splinted wounds and the body from 24 hours until the end of the experiment was highly stable. This implies the existence of a persistent volume of PIC gel in the wounds generating a consistent signal. Indeed this activity can be attributed to a thin film layer of PIC gel on the wounds in addition to gel encased within the wound bed, which is supported by histological stainings showing PIC gel in the wound area. No notable signal was detected in any distant location in the mouse other than kidneys, bladder, and liver which are involved in excretion of ^{111}In-EDTA. However, it was observed that in this wound model gel can relocate from one wound into the other (untreated) wound. The data showed that this relocation can occur both over and under the skin (see ESI Fig. S4†). In the former, an excess volume of gel combined with tight compression by the secondary dressing can cause gel to squeeze away to another location. In the latter, the wound model plays a large role. Firstly, the wounds are created by a single motion with a biopsy punch, meaning they are full thickness and connected internally. Secondly, the skin of mice is looser than that of humans.[25] Each time the mouse moves it will bend its spine, causing the loose skin of the dorsum to fold and stretch, giving the gel an opportunity to move. These factors are expected to be less problematic in human patients, where the skin is tight and wounds are more often partial-thickness.

Moreover, a large portion of the activity was detected topically on the mouse in both SPECT/CT scans and bio-distribution analysis. It is likely that the labelled PIC gel moves underneath the secondary dressing (but over the skin) as a result of behavioural activity of the mouse. Most of the hot spots outside of the wounds identified earlier on the SPECT/CT scans could be observed as key areas under the secondary dressing. For example, gel was visually observed to accumulate in the hair near the shoulders and lower back. These positions were located at the edge of the area that was shaved before surgery and were coincidentally also localized around the edge of the secondary dressings. For the intended clinical application, the movement of gel on top of the skin is not expected to be an issue as long as a sufficient amount remains on the wounds. The use of a larger animal, such as the pig, or a single injury model may be beneficial for keeping the wound dressing where it is applied. Furthermore, after careful observation of PIC treated wounds, it became apparent that the full-thickness defect fills up with the gel and that any excessive amount will spread over the skin. Reducing the applied volume is therefore advisable (in this study an ample amount was chosen intentionally to ensure full coverage). Lastly, it must be stressed that the full-thickness wound model is a stringent wound healing model, where cells can only migrate from the wound edges. In the clinic most injuries are typically partial thickness, *i.e.* reaching only partially into the dermis. This allows repopulation of the wounds from the edges as well as epidermal/stem cell sources located below, including from hair follicles and sweat glands.[26] In the full-thickness model the injury reaches into the adipose tissue and muscle, which coincidentally allows PIC gel to penetrate into the deeper layers. Furthermore, the skin of the mouse is much looser than that of humans, which increases the likelihood of gel escaping into the subcutaneous areas while the wounds are still fully open. Indeed it has been noted that there can be notable differences in the outcome of wound healing studies performed in humans compared to rodents.[25] Therefore wound healing follow-up studies often involve pigs due to their skin being more comparable to that of humans, as well as offering the possibility of studying partial thickness injuries.

In addition to studying the location of PIC in/on the body, the influence of this material on wound healing was investigated. Because the gel's impact on wound healing was only a secondary objective in this study histological observations were only made on day 7, a time point that was chosen based on SPECT imaging requirements. Macroscopic analysis revealed that the size of wounds at day 7 was similar in all conditions, including the non-splinted wounds in comparison with the splinted wounds. Non-splinted wounds typically contracted in an oval shape in concurrence with the orientation of muscle fibres, whereas splinted wounds contracted in a circular shape (see Fig. 4), which implies that the splints were functioning as intended. However, the measurements showed that wound closure by second intention (splinted) is not slower than primary intention (non-splinted) at this time point. This is in contrast with an earlier study that showed greater discrepancy between splinted and non-splinted wounds even at day 7 post injury.[27] We must stress, however, that the photographs were taken (and later analysed) with splints removed, which relaxes the skin and could make wounds appear smaller than they are in the splinted state.

Concurring with the persistent ^{111}In signal originating from the wounds, PIC gel was also observed in histological sections. However, even though several histological sections show a clear layer of PIC gel on top of the healing wound, several sections displayed encapsulation of the gels in relatively large compartments. No signs of foreign body responses against the gels have been noted (*e.g.* by a lack of giant cells) and this further supports the notion that PIC gels are not harmful, at

least up to 7 days. A future study will investigate the consequences of gel encapsulation and non-degradability of the gel at longer exposure times. This study will also investigate ways to prevent this encapsulation by mimicking a clinical scenario in which wound dressings are refreshed regularly. Moreover, one wound displayed elevated granulocyte markers but no other signs of infection, which makes it likely this increase was not related to the treatment conditions. Cells appear to grow around the hydrogel and do not enter the polymer network. This can be attributed to the small pore size of the gel and possible inability of cells to bind to the PIC. In three wounds a clear layer of granulocytic debris was detected between the wound and hydrogel. These results support our previous suggestion that PIC gels can physically block bacteria and help reduce the chance of wound infection.[11] Future work will attempt to further elucidate the ability of micro-organisms to move through PIC networks by way of microbe penetration tests.[28,29] Currently, the persistence of a layer of gel during histological processing demonstrates that the PIC gels could fulfil the absorptive quality of a wound dressing by collecting inflammatory debris.

Although many new insights were gained in the behaviour of PIC gel in full thickness wounds this study suffered from several limitations. Gel leaking out of the wound could have been partially prevented by reducing the applied volume. In addition, it is advisable to employ the same treatment conditions on wounds on the same mouse to avoid cross-contamination by leaked gel. More attention should be paid to fixation of the splints and photography of the wounds in the splinted, rather than relaxed, state. Furthermore, it was decided that imaging beyond 7 days would not be worthwhile as the activity would decay below measurable levels. This limited the extent of our histological investigation. Lastly, even though visual observation and histological investigation supported that the gel was still intact as a thin film layer at the end of the treatment it is currently still unclear if this layer is sufficient to act as stand-alone wound dressing.

Although, PIC gels are stable for at least 7 days the wound may benefit more from regular removal and re-application of the PIC dressing (*e.g.* daily or every other day) to remove the collected exudates and prevent maceration and bacterial proliferation.[30] Therefore, our upcoming study will use the SPECT/CT imaging method to quantify the efficiency of removing gel from wounds by rinsing with cold saline and confirm with histology if this can prevent gel encapsulation and improve the quality of wound repair tissue. The PIC dressings appear to fulfil the primary purposes of a wound dressing, such as protection against pathogens, hydration, and absorption of exudates. Furthermore, the results of this study provide new insights in possible future diagnostic and therapeutic applications of PIC, as functionalization of the PIC molecule is very flexible and the material itself may easily be injected.[31] This functionalization can potentially entail the incorporation of antibacterial silver ions in the DTPA groups on the PIC polymer in a similar fashion as indium.[32,33] In summary, we have shown that PIC gels remain in wounds for clinically relevant times. This opens the way for a more clinically advanced bio-functional wound dressing that is both convenient and can be tailored to a patient's specific needs.

5. Conclusion

This study demonstrated (1) the convenient functionalization of PIC polymer with new functional molecules for labelling and tracing. This also implies a possible application for PIC as diagnostic or therapeutic method. In addition, (2) it was discovered that it is not likely for PIC to enter the bloodstream or through other means reach distant locations in the body but stays localized at the site of application (*i.e.* the wounds and surrounding skin) for at least 7 days. Furthermore, it was found that PIC gels were contained inside the humanized full-thickness wound model for clinically relevant times and were practical to use due to their thermo-reversible nature, adherent strength, and stability. Taken together, our results imply that PIC hydrogels are suitable for further developing into a clinically usable wound cover.

Conflicts of interest

Author AER is inventor of patents regarding the preparation and use of the PIC gel (#EP2287221, EP3021872, WO2017037293). Author OIvdB works for NovioCell BV which produces PIC polymers.

Acknowledgements

We acknowledge Ewald Bronkhorst for his input in performing the statistical analysis and the department of Pathology of the Radboudumc (Nijmegen, the Netherlands) for imaging of the histological slides. This project was funded by ZonMW (Biomimetic Hydrogel allowing customizable Wound Care # 436001005).

References

1 M. D. Peck, Epidemiology of burns throughout the world. Part I: Distribution and risk factors, *Burns*, 2011, **37**(7), 1087–1100.
2 M. M. Rybarczyk, J. M. Schafer, C. M. Elm, S. Sarvepalli, P. A. Vaswani, K. S. Balhara, *et al.*, Prevention of burn injuries in low- and middle-income countries: A systematic review, *Burns*, 2016, **42**(6), 1183–1192.
3 B. S. Atiyeh, M. Costagliola and S. N. Hayek, Burn prevention mechanisms and outcomes: pitfalls, failures and successes, *Burns*, 2009, **35**(2), 181–193.
4 H. Hollinworth and M. Collier, Nurses' views about pain and trauma at dressing changes: results of a national survey, *J. Wound Care*, 2000, **9**(8), 369–373.

5 J. Qu, X. Zhao, Y. Liang, T. Zhang, P. X. Ma and B. Guo, Antibacterial adhesive injectable hydrogels with rapid self-healing, extensibility and compressibility as wound dressing for joints skin wound healing, *Biomaterials*, 2018, **183**, 185–199.
6 J. S. Boateng, K. H. Matthews, H. N. E. Stevens and G. M. Eccleston, Wound healing dressings and drug delivery systems: A review, *J. Pharm. Sci.*, 2008, **97**(8), 2892–2923.
7 W. H. Eaglstein, Moist wound healing with occlusive dressings: a clinical focus, *Dermatol. Surg.*, 2001, **27**(2), 175–182.
8 X. Zhao, H. Wu, B. Guo, R. Dong, Y. Qiu and P. X. Ma, Antibacterial anti-oxidant electroactive injectable hydrogel as self-healing wound dressing with hemostasis and adhesiveness for cutaneous wound healing, *Biomaterials*, 2017, **122**, 34–47.
9 Y. Liang, X. Zhao, T. Hu, B. Chen, Z. Yin, P. X. Ma, *et al.*, Adhesive Hemostatic Conducting Injectable Composite Hydrogels with Sustained Drug Release and Photothermal Antibacterial Activity to Promote Full-Thickness Skin Regeneration During Wound Healing, *Small*, 2019, **15**(12), 1900046.
10 S. Li, S. Dong, W. Xu, S. Tu, L. Yan, C. Zhao, *et al.*, Antibacterial Hydrogels, *Adv. Sci.*, 2018, **5**(5), 1700527.
11 R. C. op 't Veld, O. I. van den Boomen, D. M. S. Lundvig, E. M. Bronkhorst, P. H. J. Kouwer, J. A. Jansen, *et al.*, Thermosensitive biomimetic polyisocyanopeptide hydrogels may facilitate wound repair, *Biomaterials*, 2018, **181**, 392–401.
12 PH Kouwer, M Koepf, VA Le Sage, M Jaspers, AM van Buul, ZH Eksteen-Akeroyd, *et al.*, Responsive biomimetic networks from polyisocyanopeptide hydrogels, *Nature*, 2013, **493**(7434), 651–655.
13 M. Jaspers, M. Dennison, M. F. J. Mabesoone, F. C. MacKintosh, A. E. Rowan and P. H. J. Kouwer, Ultra-responsive soft matter from strain-stiffening hydrogels, *Nat. Commun.*, 2014, **5**, 5808.
14 R. K. Das, V. Gocheva, R. Hammink, O. F. Zouani and A. E. Rowan, Stress-stiffening-mediated stem-cell commitment switch in soft responsive hydrogels, *Nat. Mater.*, 2016, **15**(3), 318–325.
15 K. Liu, S. M. Mihaila, A. Rowan, E. Oosterwijk and P. H. J. Kouwer, Synthetic Extracellular Matrices with Nonlinear Elasticity Regulate Cellular Organization, *Biomacromolecules*, 2019, **20**(2), 826–834.
16 M. Jaspers, A. C. H. Pape, I. K. Voets, A. E. Rowan, G. Portale and P. H. J. Kouwer, Bundle Formation in Biomimetic Hydrogels, *Biomacromolecules*, 2016, **17**(8), 2642–2649.
17 P. Laurén, Y. R. Lou, M. Raki, A. Urtti, K. Bergström and M. Yliperttula, Technetium-99m-labeled nanofibrillar cellulose hydrogel for in vivo drug release, *Eur. J. Pharm. Sci.*, 2014, **65**, 79–88.
18 C. L. Peng, Y. H. Shih, K. S. Liang, P. F. Chiang, C. H. Yeh, I. C. Tang, *et al.*, Development of in situ forming thermosensitive hydrogel for radiotherapy combined with chemotherapy in a mouse model of hepatocellular carcinoma, *Mol. Pharm.*, 2013, **10**(5), 1854–1864.
19 Y. Kim, D. R. Seol, S. Mohapatra, J. J. Sunderland, M. K. Schultz, F. E. Domann, *et al.*, Locally targeted delivery of a micron-size radiation therapy source using temperature-sensitive hydrogel, *Int. J. Radiat. Oncol., Biol., Phys.*, 2014, **88**(5), 1142–1147.
20 R. D. Galiano, V. Michaels, M. Dobryansky, J. P. Levine and G. C. Gurtner, Quantitative and reproducible murine model of excisional wound healing, *Wound Repair Regen.*, 2004, **12**(4), 485–492.
21 X. Wang, J. Ge, E. E. Tredget and Y. Wu, The mouse excisional wound splinting model, including applications for stem cell transplantation, *Nat. Protoc.*, 2013, **8**(2), 302–309.
22 L. Dunn, H. C. G. Prosser, J. T. M. Tan, L. Z. Vanags, M. K. C. Ng and C. A. Bursill, Murine model of wound healing, JoVE, *J. Visualized Exp.*, 2013, **75**, e50265.
23 C. A. Schneider, W. S. Rasband and K. W. Eliceiri, NIH Image to ImageJ: 25 years of image analysis, *Nat. Methods*, 2012, **9**, 671.
24 S. Mandal, R. Hammink, J. Tel, Z. H. Eksteen-Akeroyd, A. E. Rowan, K. Blank, *et al.*, Polymer-Based Synthetic Dendritic Cells for Tailoring Robust and Multifunctional T Cell Responses, *ACS Chem. Biol.*, 2015, **10**(2), 485–492.
25 L. Rittié, Cellular mechanisms of skin repair in humans and other mammals, *J. Cell Commun. Signal.*, 2016, **10**(2), 103–120.
26 G. Taylor, M. S. Lehrer, P. J. Jensen, T.-T. Sun and R. M. Lavker, Involvement of Follicular Stem Cells in Forming Not Only the Follicle but Also the Epidermis, *Cell*, 2000, **102**(4), 451–461.
27 N. A. J. Cremers, M. Suttorp, M. M. Gerritsen, R. J. Wong, C. van Run-van Breda, G. M. van Dam, *et al.*, Mechanical Stress Changes the Complex Interplay Between HO-1, Inflammation and Fibrosis, During Excisional Wound Repair, *Front. Biomed.*, 2015, **2**(86), DOI: 10.3389/fmed.2015.00086.
28 M. T. Razzak, D. Darwis and S. Zainuddin, Irradiation of polyvinyl alcohol and polyvinyl pyrrolidone blended hydrogel for wound dressing, *Radiat. Phys. Chem.*, 2001, **62**(1), 107–113.
29 Z. Ajji, I. Othman and J. M. Rosiak, Production of hydrogel wound dressings using gamma radiation, *Nucl. Instrum. Methods Phys. Res., Sect. B*, 2005, **229**(3), 375–380.
30 S. Dhivya, V. V. Padma and E. Santhini, Wound dressings - a review, *Biomedicine*, 2015, **5**(4), 22.
31 B. Wang, J. Shao, J. A. Jansen, X. F. Walboomers and F. Yang, A Novel Thermoresponsive Gel as a Potential Delivery System for Lipoxin, *J. Dent. Res.*, 2019, **98**(3), 355–362.
32 C. De Stefano, G. Lando, A. Pettignano and S. Sammartano, Evaluation of the sequestering ability of different complexones towards Ag^+ ion, *J. Mol. Liq.*, 2014, **199**, 432–439.
33 D. J. Leaper, Silver dressings: their role in wound management, *Int. Wound J.*, 2006, **3**(4), 282–294.

